RESEARCH ARTICLE
SPACE PHYSICS: MAGNETOSPHERIC PHYSICS

Earth and Planetary Physics
8: 368–374, 2024
doi: 10.26464/epp2024001

A statistical analysis of the Kappa-type energy spectrum distribution of radiation belt electrons observed by Van Allen Probes

LuHuai Jiao, Xin Ma*, YuanNong Zhang, TaiFeng Jin, Song Fu, and BinBin Ni

Department of Space Physics, School of Electronic Information, Wuhan University, Wuhan 430072, China

Key Points:

- The Kappa-type distribution is applied to fit electron flux data from the Van Allen Probes at L = 4–6 under different geomagnetic conditions.
- The Kappa-type distribution performs better at the higher L-shells (L ~ 5–6) when the geomagnetic condition is relatively active.
- The typical radiation belt electron energy spectra can easily be constructed by using the fitting parameters.

Citation: Jiao, L. H., Ma, X., Zhang, Y. N., Jin, T. F., Fu, S., and Ni, B. B. (2024). A statistical analysis of the Kappa-type energy spectrum distribution of radiation belt electrons observed by Van Allen Probes. *Earth Planet. Phys.*, *8*(2), 368–374. http://doi.org/10.26464/epp2024001

Abstract: The energy spectrum of energetic electrons is a key factor representing the dynamic variations of Earth's Van Allen radiation belts. Increased measurements have indicated that the commonly used Maxwellian and Kappa distributions are inadequate for capturing the realistic spectral distributions of radiation belt electrons. Here we adopt the Kappa-type (KT) distribution as the fitting function and perform a statistical analysis to investigate the radiation belt electron flux spectra observed by the Van Allen Probes. By calculating the optimal values of the key KT distribution parameters (i.e., κ and θ^2) from the observed spectral shapes, we fit the radiation belt electron fluxes at different L-shells under different geomagnetic conditions. In this manner, we obtain typical values of the KT distribution parameters, which are statistically feasible for modeling the radiation belt electron flux profiles during either geomagnetically quiet or active periods. A comparison of the KT distribution model results with those using the Maxwellian or Kappa distribution reveals the advantage of the KT distribution for studying the overall properties of the radiation belt electron spectral distribution, which has important implications for deepening the current understanding of the radiation belt electron dynamics under evolving geomagnetic conditions.

Keywords: radiation belt electron; Kappa-type distribution; fitting; geomagnetic storm

1. Introduction

The distribution of electron fluxes in the Earth's radiation belts is essential for understanding various associated physical processes. Energetic electrons in the Earth's radiation belts, often called "killer electrons" because of their destructive energy capable of causing malfunctions of orbiting spacecrafts, play an important role in space plasma dynamics (e.g., Baker, 2002). Energetic electron fluxes in the outer radiation belt are highly variable (e.g., Li XL et al., 1997; Reeves et al., 1998, 2003; Zong QG et al., 2007), which makes them difficult to describe accurately. The Maxwellian distribution function was widely adopted in early studies, until a non-Maxwellian tail in the distribution at the high-energy end (e.g., Vasyliunas, 1968; Leubner, 1982) was generally observed by particle detectors in the natural space environment, indicating a thermal nonequilibrium state of space plasmas. A useful function for fitting such plasma distributions is the generalized Lorentzian (Kappa) distribution (Vasyliunas, 1968; Christon et al., 1988; Summers and Thorne, 1992; Viñas et al., 2005), which can properly describe the observed high-energy tail by introducing the parameter κ. When $\kappa \to \infty$, the Kappa distribution approaches the Maxwellian distribution. The typical Kappa distribution has since been widely used in various studies (e.g., Xue S et al., 1993; Maksimovic et al., 1997a, b; Saito et al., 2000; Dasso et al., 2003; Cao X et al., 2020; Lou YQ et al., 2023).

Despite its popularity, the Kappa distribution still shows recognizable differences, especially when modeling electron spectra in the high energy range. As an important step toward improvement, Xiao FL (2006) developed a Kappa-type (KT) distribution to model the high-energy tail distribution in a more appropriate way. The KT distribution satisfies the power law not only at the lower energies, but also at the relativistic energies, whereas the Kappa distribution decreases faster than the KT distribution with increasing

First author: H. L. Jiao, jiaoluhuai@whu.edu.cn
Correspondence to: X. Ma, whumaxin@whu.edu.cn
Received 01 AUG 2023; Accepted 26 OCT 2023.
First Published online 29 NOV 2023.

kinetic energy. Some studies have been conducted on the application of the KT distribution. Xiao FL et al. (2017) studied the generation of extremely low frequency chorus waves in the Van Allen radiation belts. Yang QW et al. (2016) examined the magnetospheric chorus wave instability induced by relativistic KT distributions. By comparing the modeled electron fluxes using the KT distribution with the observational data from a geostationary-orbit satellite at different universal times, Xiao FL et al. (2008) concluded that the KT distribution is a more reasonable way to fit highly energetic particles. It is worth noting that the results of Xiao FL et al. (2008) apply only to the region of the geostationary orbit. Therefore, it is valuable to attempt to investigate the applicability of the KT distribution for modeling the electron energy spectra in other regions of the radiation belt. The high-quality electron datasets provided by the twin Van Allen Probes (VAP) provide such an opportunity.

The outline of this paper is as follows. In Section 2, we briefly describe the KT distribution model and the electron flux data obtained from the VAP. In Section 3, we fit the flux data by using the KT distribution, Kappa distribution, and Maxwellian distribution and compare the results. On the basis of the KT distribution fitting technique, we show the best fitting parameters for electron flux at L = 4–6 under different geomagnetic conditions. The performance of the modeled electron flux depending on the KT function is summarized and discussed in Section 4.

2. Fitting Method and Data

2.1 The KT Distribution Function

The relation between the differential flux $j(E)$ and the distribution function $f(p)$ can be written as (Schulz and Lanzerotti, 1974)

$$j(E) = p^2 f(p), \tag{1}$$

where E is the kinetic energy of particles and p is the momentum of particles. To simplify the calculation, variables are normalized in the following way: $p_s = p/m_0c$; $E_s = E/E_0$, where $E_0 = m_0c^2$, m_0 is the electron rest mass, and c is the speed of light. The relativistic KT distribution can then be written as (Xiao FL et al., 2008)

$$f^{KT}(p_s, \alpha) = \frac{N}{2\pi^{3/2}} \frac{\Gamma((q+3)/2)}{\Gamma((q+2)/2)} \frac{1}{I} \left(1 + \frac{\sqrt{1+p_s^2}-1}{\kappa\theta^2}\right)^{-(\kappa+1)} \sin^q\alpha, \tag{2}$$

where I is the constant for normalization as

$$I = \frac{8B(3/2, \kappa-2)}{2\kappa-1}\left[3F(\kappa+1, 5/2; \kappa+1/2; 1-2/\kappa\theta^2) + (\kappa-2)F(\kappa+1, 3/2; \kappa+1/2; 1-2/\kappa\theta^2)\right],$$

here Γ, B, and F represent the gamma function, the beta function, and the hypergeometric function, respectively; N is the number density of particles; α is the particle pitch angle; q represents the pitch angle anisotropy; and θ^2 represents the thermal energy scaled by E_0.

In this study, we focus only on those electrons with a pitch angle of 90° and ignore the pitch angle anisotropy. With p_s rewritten as p, the relativistic KT distribution can be written as

$$f(p) = \frac{N}{4\pi I}\left(1 + \frac{\sqrt{1+p^2}-1}{\kappa\theta^2}\right)^{-(\kappa+1)}. \tag{3}$$

The normalized relation between the differential flux $j(E)$ and the distribution function $f(p)$ can be written as

$$j = \frac{cE_s(E_s+2)}{E_0} f(p). \tag{4}$$

2.2 Data Sets

The VAP mission was launched on August 30, 2012, into an orbit with a perigee of ~1.1 R_E, an apogee of ~6 R_E, an inclination of 10.2°, and an orbital period of ~9 hours. It consists of two satellites, Van Allen Probe A (VAP-A) and Van Allen Probe B (VAP-B). The primary objective of this mission is to understand the fundamental physics of the radiation belts (Mauk et al., 2013). The Energetic Particle, Composition, and Thermal Plasma Suite (ECT) carried by the VAP is designed to measure various kinds of particles in the radiation belts. The ECT is a set of instruments, among which the Magnetic Electron Ion Spectrometer (MagEIS; Claudepierre et al., 2015) and the Relativistic Electron Proton Telescope (REPT; Baker et al., 2021) are for electron measurements. The MagEIS observes electrons in the middle energy ranges, from ~30 to ~3800 keV, whereas the REPT observes electrons in the relativistic energy ranges, from 1.8 to 20 MeV. The ECT provides high-resolution (11 seconds per sample) electron flux data, which covers almost all pitch angles.

In this study, we use the electron spectrum dataset measured by the MagEIS and REPT, covering the time range from January 1, 2013, to December 31, 2016. The magnetic field is sensitive to geomagnetic activity. In this study, we use the L data provided by the ECT suite of the VAP. Only those spectra sampled at L = 4 ± 0.1, 4.5 ± 0.1, 5 ± 0.1, 5.5 ± 0.1, and 6 ± 0.1 are selected. We further categorize the samples into a quiet period and an active period according to the geomagnetic activity index SYM-H. A value of SYM-H greater than −30 nT indicates a geomagnetically quiet period (Gonzalez et al., 1994). For a given distribution function, the fitting of a spectrum is performed by using the least squares method.

3. Analytical Results

3.1 Comparison Between Different Distribution Functions

To examine the performance of the KT distribution, we compare the fitting results of the VAP-observed electron flux by using the Maxwellian, Kappa, and KT distributions, as shown in Figure 1. Two spectrum samples under different geomagnetic conditions, the quiet period and the active period, are arbitrarily selected for testing. In Figure 1a, the fitting parameter for the Maxwellian distribution is θ^2 = 0.06, the fitting parameter for the Kappa distribution is κ = 3, θ^2 = 0.035, and the fitting parameter for the KT distribution is κ = 6, θ^2 = 0.05. Similarly, in Figure 1b, the fitting parameter for the Maxwellian distribution is θ^2 = 0.09, the fitting parameter for the Kappa distribution is κ = 4, θ^2 = 0.32, and the fitting parameter for the KT distribution is κ = 9, θ^2 = 0.15. We see from the figure that the Maxwellian distribution fails to describe the observed high-energy electrons in both cases, whereas the

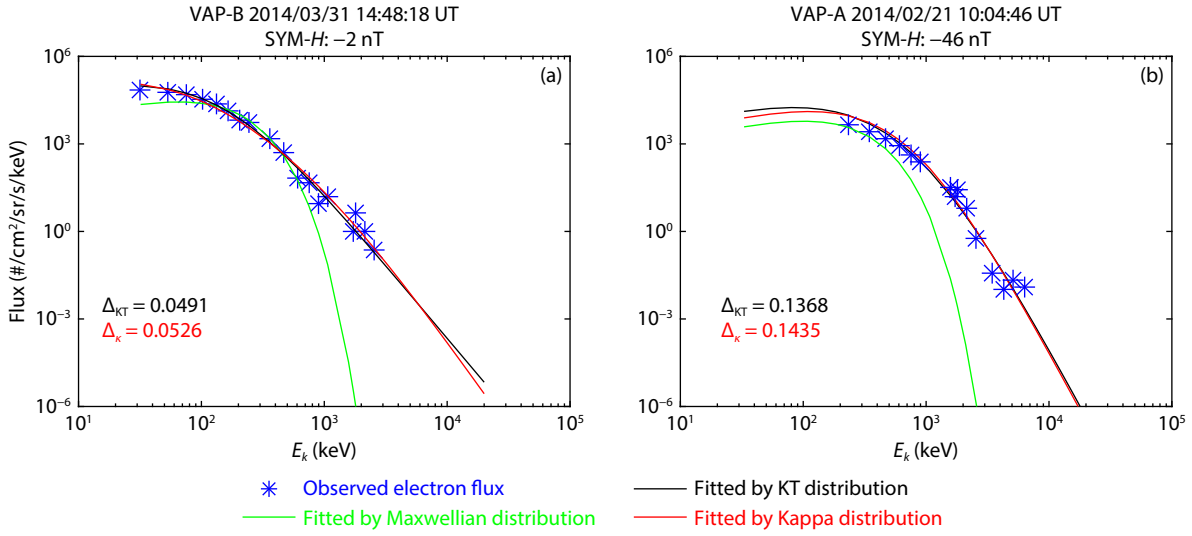

Figure 1. The fitting results for electron flux when using the Maxwellian, Kappa, and Kappa-type (KT) distribution under two different geomagnetic conditions: (a) SYM-H = 2 nT on March 31, 2014, at 14:48:18 universal time (UT), quiet period; (b) SYM-H = −46 nT on February 21, 2014, at 10:04:46 UT, active period. The blue asterisks represent the electron flux data observed by the MagEIS and REPT onboard the VAP-A and VAP-B. The green curves are fittings by the Maxwellian distribution, the black curves represent fittings by the KT distribution, and the red curves represent fittings by the Kappa distribution. Δ_{KT} is the difference between observations and the KT distribution fittings, and Δ_κ is the difference between observations and the Kappa distribution fittings.

Kappa and KT distributions fit the observations well through all the energy scales. A sum of several Maxwellian distributions can probably also describe the observation well. However, such a fitting method is commonly indirect and more complicated than fitting by the KT distribution. To further quantify the performance of the latter two distributions, we calculate the differences between fittings and observations, Δ_κ for the Kappa distribution and Δ_{KT} for the KT distribution. In both cases, Δ_{KT} is slightly smaller than Δ_κ, suggesting that the KT distribution is a better function for describing the electron flux in the radiation belts.

3.2 Parametric Fitting

We then analyze the values of parameters in the KT distribution. According to the description in Section 2.1, the key parameters of the distribution are κ and θ^2, which fundamentally determine the shape of the distribution function. For every electron spectrum sample, a pair of values (κ, θ^2) is obtained by fitting. The fitting procedure is designed to return κ as an integer between 3 and 12 and θ^2 as an exact multiple of 0.005 between 0.005 and 0.4. The ranges of κ and θ^2 are selected based on previous studies. All possible pairs of (κ, θ^2) form a two-dimensional grid. We count the number of samples matching each grid point and calculate the average value of the differences. It is obvious that a higher count of samples for a given pair of values means better applicability of the distribution function with such parameters (i.e., fits with more cases [samples]). On the other hand, a smaller difference between the fitting curve and the measurement indicates better accuracy of the distribution. We intend to find the optimal values of parameters (i.e., a pair of values that can satisfy both the applicability and accuracy appropriately).

Figure 2 shows the fitting results of the KT distribution (left column) at L = 6 under the quiet geomagnetic condition. The results of the Kappa distribution are also shown for comparison. Figures 2a and 2c show the number of samples fitted by the KT distribution and the Kappa distribution, respectively, in the κ–θ^2 plane. One can easily see the concentration of samples along a diagonal line in Figure 2a, whereas in Figure 2c the samples are distributed mainly at κ = 3, the boundary of the grid. Such results are usually considered unreasonable. Figures 2b and 2d show the average differences in the fittings by the KT distribution and the Kappa distribution in the κ–θ^2 plane. Compared with 2a, in Figure 2b one can see that the differences at the most concentrated grids are all below 0.3, whereas in Figure 2d, the differences reach nearly 0.4 for the most concentrated grids. This result confirms that from the case study presented in Section 3.1.

In Figure 2a, it is interesting to see how the samples are concentrated not at a single point but along a diagonal line. Hence, we try to find the line of typical parameters, each point on which corresponds to a pair of typical values that are equally applicable to fit the electron spectra. To do so, we apply several criteria to select those grids with the most samples. After removing unreliable values at the boundary of the grid, we select only the grid points with counts of samples exceeding 0.5% of the total, and with differences below 0.25. The parameters of selected grids are weighted by their count values and fitted by the least squares line with the slope a and the y-intercept b.

Figures 3 and 4 show the counts of samples, the averaged differences, and the fitted lines of typical parameters over selected grids at five different L-shell regions under geomagnetically quiet and active periods, respectively. One can see from the two figures that under the same geomagnetic condition, the difference increases as L decreases. The best result is obtained at L = 6, meaning that the electron spectra are better described by the KT distribution at a higher L-shell. On the other hand, by comparing

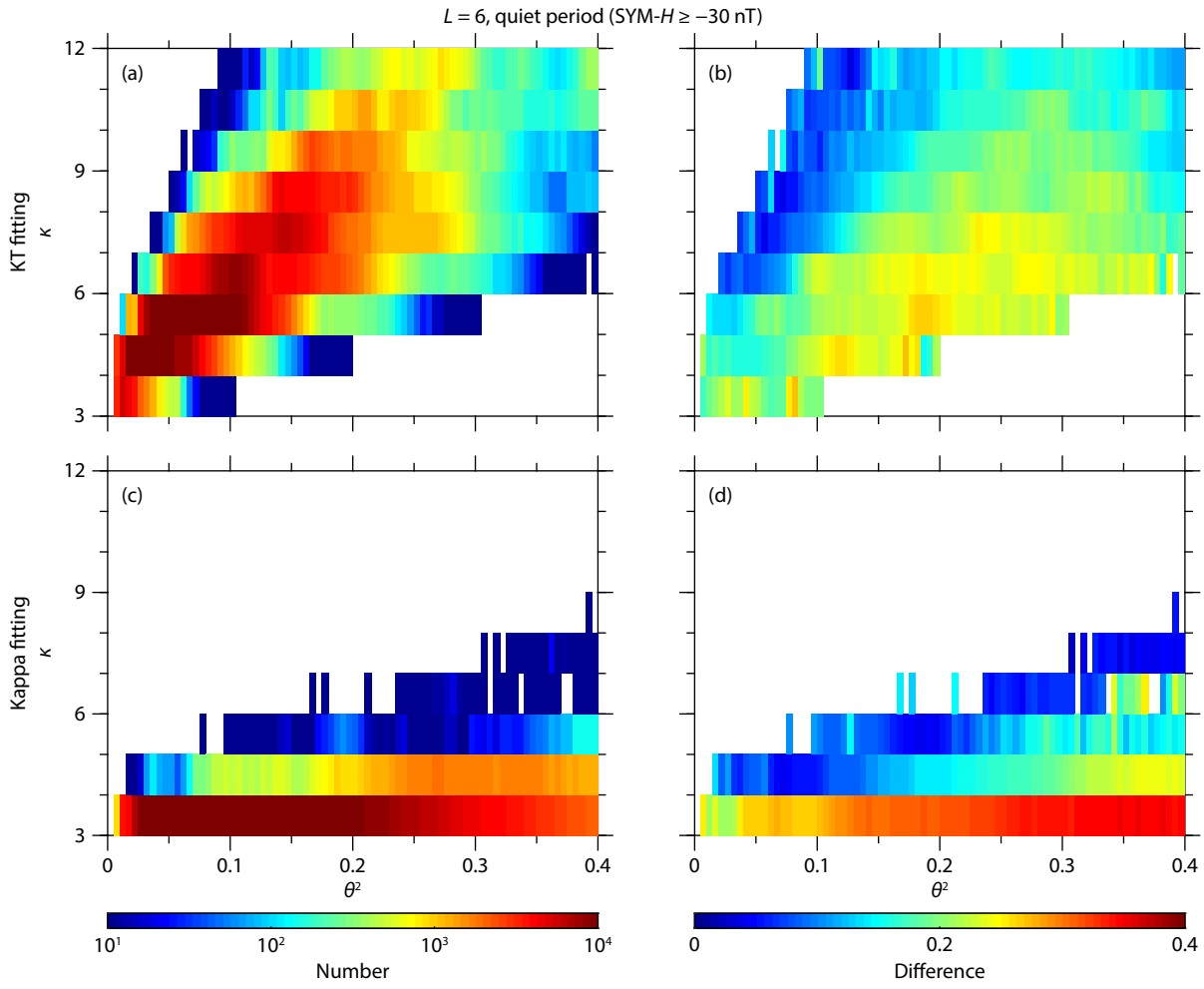

Figure 2. Fitting results of (a, b) the Kappa-type (KT) function and (c, d) the Kappa function at $L = 6$ under the quiet geomagnetic condition.

the results at the same L-shell region, one can see that the averaged differences under the active geomagnetic condition are lower than those under the quiet geomagnetic condition, which suggests that the electron spectra are better described by the KT distribution under the more active geomagnetic condition.

Table 1 shows the fitting parameters of lines of typical parameters from the results of the KT distribution, a and b, together with the applicable range of κ and the well-fitting rate, under quiet and active geomagnetic conditions, respectively. We define the well-fitting case as the fitting result of a sample spectrum whose difference is lower than 0.40. The well-fitting rate, introduced to evaluate the performance of the KT distribution determined by typical parameters, is hence defined as the number of well-fitting cases divided by the total number of cases. The well-fitting rate shows the overall performance of the KT distribution with typical parameters. From the table, we can see that the performance of the KT distribution is better at the higher L-shell ($L \sim 5$–6) regions when the geomagnetic condition is relatively active.

4. Concluding Remarks

In this study, using the electron flux data from the VAP, we have examined the performance of the Maxwellian, Kappa, and KT distributions in fitting the energy spectra of electrons in the radiation belts and have optimized the fitting parameters of the KT distribution at different L-shells under different geomagnetic conditions. Our results indicate the advantage of the KT distribution, compared with the Maxwellian and Kappa distributions, in accurately fitting the high-energy tail of electron spectra. With the availability of a 4-year high-quality electron spectrum dataset, we have found a number of parameter value pairs aligned to straight lines that can fit reasonably well with the majority of the observation samples. In addition, we have witnessed better performance of the KT distribution for fitting of the electron energy spectrum at larger L-shells (i.e., $L \sim 5$–6) during active geomagnetic periods, which is consistent with the conclusion of Xiao FL et al. (2008). As a consequence, our results have important implications for deepening the current understanding of the radiation belt electron dynamics under evolving geomagnetic conditions.

It is also worth noting that no single pair of parameters is identified for any given L-shell or geomagnetic condition. As shown in Figures 3 and 4, the counts of samples corresponding to the pairs of values do not concentrate on individual points but on the diagonal lines instead. This result implies that no single parameter or pair of parameters is suitable for describing all observed radiation belt electron spectra. Nevertheless, we have attempted to use the least parameters possible for fits and have found that no more than 4 points on the κ–θ^2 plane (i.e., 4 pairs of values) are sufficient to properly model the majority of observed electron flux spectra.

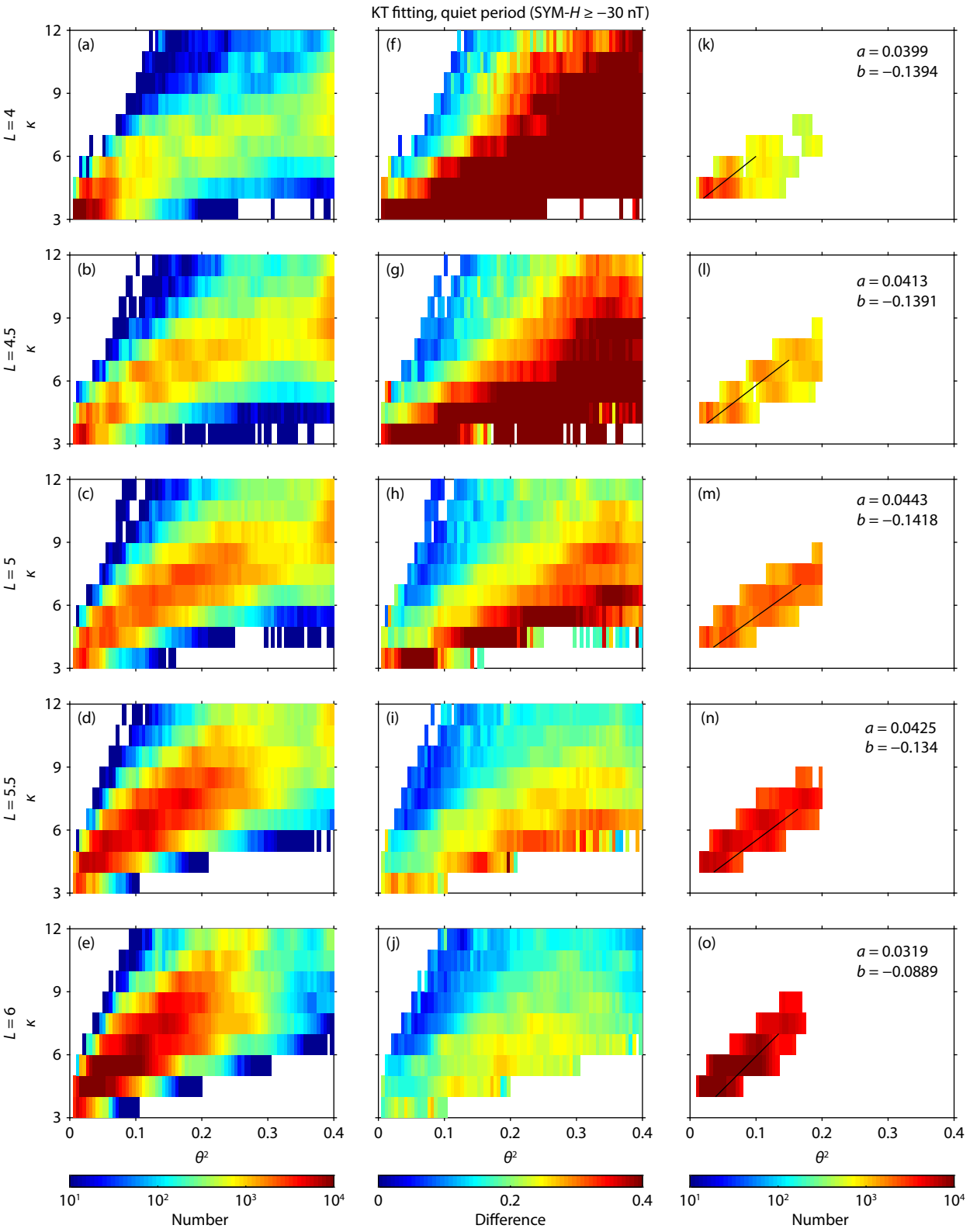

Figure 3. Fitting results of different pairs of parameter values under the quiet geomagnetic condition at L = 4 to 6. (a)–(e) Number of cases; (f)–(j) averaged differences; (k)–(o) linear fitting of parameters using selected cases with high count numbers and low differences.

The parameters of fitting lines for these points are listed in Table 1, which can be readily adopted to establish the typical radiation belt electron energy spectra for future simulations of radiation belt electron variations under a variety of magnetospheric circumstances.

Acknowledgements

This work was supported by the National Natural Science Founda-

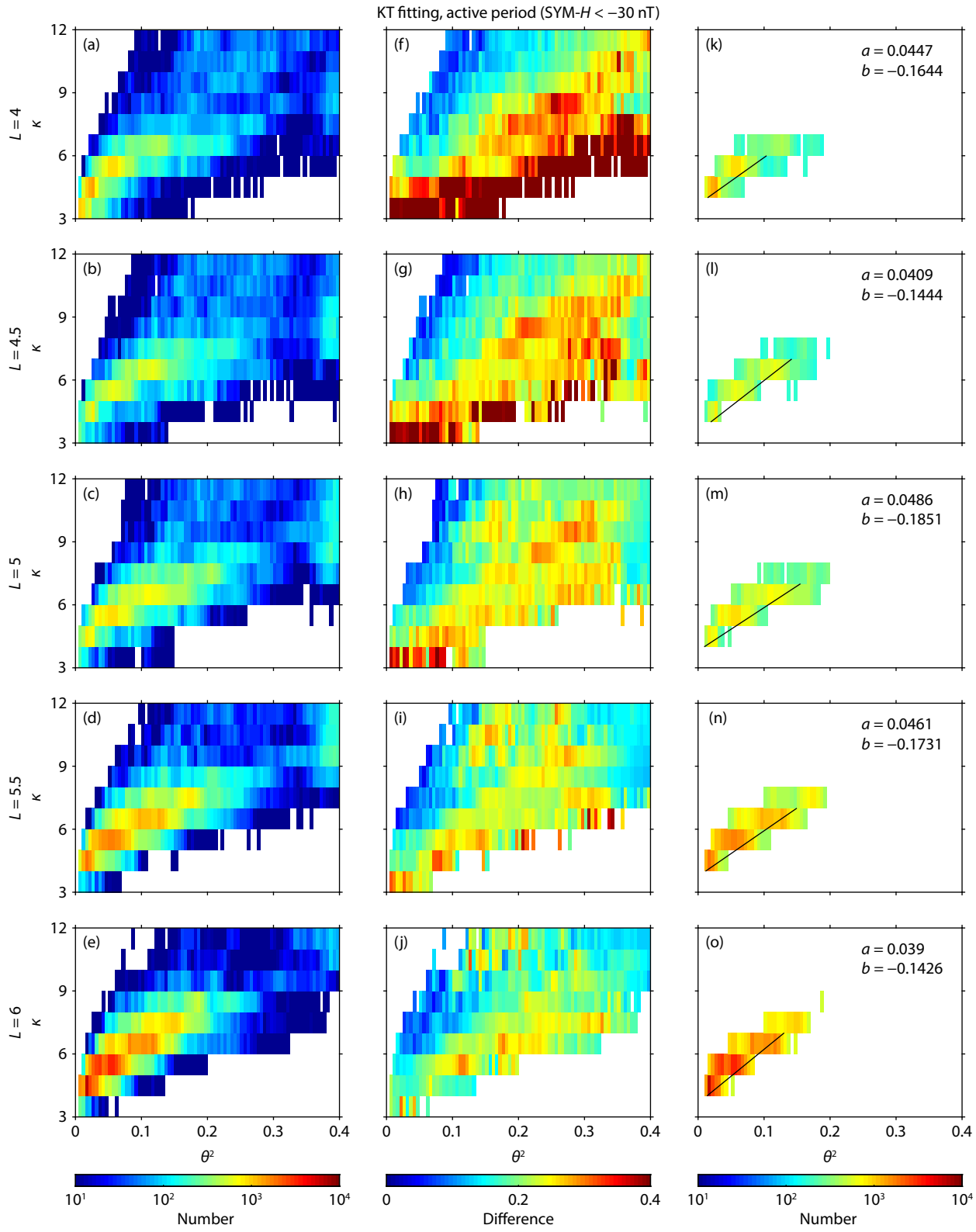

Figure 4. Fitting results of different pairs of parameter values under the active geomagnetic condition at L = 4 to 6. The format is the same as for Figure 3.

tion of China (Grant Nos. 42188101, 42025404, 41974186, 42174188, and 42204160), the National Key R&D Program of China (Grant No. 2022YFF0503700), the B-type Strategic Priority Program of the Chinese Academy of Sciences (Grant No. XDB41000000), the Fundamental Research Funds for the Central Universities (Grant Nos. 2042022kf1016 and 2042023kf1025), and the China Postdoctoral Science Foundation (Grant No. 2022M722447). We also acknowledge the Van Allen Probes mission, particularly the ECT team, for providing particle data. The electron flux data were obtained from http://www.rbsp-

Table 1. Lines of typical parameters and their applicable ranges.

L	Quiet time			Active time		
	Line of typical parameters[a]	Range of κ	Well-fitting rate (%)	Line of typical parameters	Range of κ	Well-fitting rate (%)
4	(0.0399, −0.1394)	[4, 6]	19.18	(0.0447, −0.1644)	[4, 6]	52.90
4.5	(0.0413, −0.1391)	[4, 7]	25.56	(0.0409, −0.1444)	[4, 7]	50.52
5	(0.0443, −0.1418)	[4, 7]	48.43	(0.0486, −0.1851)	[4, 7]	60.32
5.5	(0.0425, −0.1340)	[4, 7]	69.32	(0.0461, −0.1731)	[4, 7]	71.85
6	(0.0319, −0.0889)	[4, 7]	79.32	(0.0390, −0.1426)	[4, 7]	81.14

[a]A pair of values (a, b) indicates a line $\theta^2 = a\kappa + b$ fitting typical parameters on the κ–θ^2 grid within the declared range of κ.

ect.lanl.gov/data_pub/. The geomagnetic indices were obtained online from the OMNIWeb (http://omniweb.gsfc.nasa.gov/).

References

Baker, D. N. (2002). How to cope with space weather. *Science*, *297*(5586), 1486–1487. https://doi.org/10.1126/science.1074956

Baker, D. N., Kanekal, S. G., Hoxie, V., Li, X. L., Jaynes, A. N., Zhao, H., Elkington, S. R., Foster, J. C., Selesnick, R., ... Filwett, R. (2021). The Relativistic Electron–Proton Telescope (REPT) investigation: Design, operational properties, and science highlights. *Space Sci. Rev.*, *217*(5), 68. https://doi.org/10.1007/s11214-021-00838-3

Cao, X., Ni, B. B., Summers, D., Ma, X., Lou, Y. Q., Zhang, Y., Gu, X. D., and Fu, S. (2020). Effects of superthermal plasmas on the linear growth of multiband EMIC waves. *Astrophys. J.*, *899*(1), 43. https://doi.org/10.3847/1538-4357/ab9ec4

Christon, S. P., Mitchell, D. G., Williams, D. J., Frank, L. A., Huang, C. Y., and Eastman, T. E. (1988). Energy spectra of plasma sheet ions and electrons from ~50 eV/*e* to ~1 MeV during plasma temperature transitions. *J. Geophys. Res.: Space Phys.*, *93*(A4), 2562–2572. https://doi.org/10.1029/JA093iA04p02562

Claudepierre, S. G., O'Brien, T. P., Blake, J. B., Fennell, J. F., Roeder, J. L., Clemmons, J. H., Looper, M. D., Mazur, J. E., Mulligan, T. M., ... Larsen, B. A. (2015). A background correction algorithm for Van Allen Probes MagEIS electron flux measurements. *J. Geophys. Res.: Space Phys.*, *120*(7), 5703–5727. https://doi.org/10.1002/2015JA021171

Dasso, S., Gratton, F. T., and Farrugia, C. J. (2003). A parametric study of the influence of ion and electron properties on the excitation of electromagnetic ion cyclotron waves in coronal mass ejections. *J. Geophys. Res.: Space Phys.*, *108*(A4), 1149. https://doi.org/10.1029/2002JA009558

Gonzalez, W. D., Joselyn, J. A., Kamide, Y., Kroehl, H. W., Rostoker, G., Tsurutani, B. T., and Vasyliunas, V. M. (1994). What is a geomagnetic storm?. *J. Geophys. Res.: Space Phys.*, *99*(A4), 5771–5792. https://doi.org/10.1029/93JA02867

Leubner, M. P. (1982). On Jupiter's whistler emission. *J. Geophys. Res.: Space Phys.*, *87*(A8), 6335–6338. https://doi.org/10.1029/JA087iA08p06335

Li, X. L., Baker, D. N., Temerin, M., Cayton, T. E., Reeves, E. G. D., Christensen, R. A., Blake, J. B., Looper, M. D., Nakamura, R., and Kanekal, S. G. (1997). Multisatellite observations of the outer zone electron variation during the November 3–4, 1993, magnetic storm. *J. Geophys. Res.: Space Phys.*, *102*(A7), 14123–14140. https://doi.org/10.1029/97JA01101

Lou, Y. Q., Cao, X., Wu, M. Y., Ni, B. B., and Zhang, T. L. (2023). Scalings for the Alfvén-cyclotron instability in a bi-kappa plasma. *Earth Planet. Phys.*, *7*(6), 1–9. https://doi.org/10.26464/epp2023080

Maksimovic, M., Pierrard, V., and Lemaire, J. F. (1997a). A kinetic model of the solar wind with Kappa distribution functions in the corona. *Astron. Astrophys.*, *324*(2), 725–734

Maksimovic, M., Pierrard, V., and Riley, P. (1997b). Ulysses electron distributions fitted with Kappa functions. *Geophys. Res. Lett.*, *24*(9), 1151–1154. https://doi.org/10.1029/97GL00992

Mauk, B. H., Fox, N. J., Kanekal, S. G., Kessel, R. L., Sibeck, D. G., and Ukhorskiy, A. (2013). Science objectives and rationale for the radiation belt storm probes mission. *Space Sci. Rev.*, *179*(1-4), 3–27. https://doi.org/10.1007/s11214-012-9908-y

Reeves, G. D., Friedel, R. H. W., Belian, R. D., Meier, M. M., Henderson, M. G., Onsager, T., Singer, H. J., Baker, D. N., Li, X., and Blake, J. B. (1998). The relativistic electron response at geosynchronous orbit during the January 1997 magnetic storm. *J. Geophys. Res.: Space Phys.*, *103*(A8), 17559–17570. https://doi.org/10.1029/97JA03236

Reeves, G. D., McAdams, K. L., Friedel, R. H. W., and O'Brien, T. P. (2003). Acceleration and loss of relativistic electrons during geomagnetic storms. *Geophys. Res. Lett.*, *30*(10), 1529. https://doi.org/10.1029/2002GL016513

Saito, S., Forme, F. R. E., Buchert, S. C., Nozawa, S., and Fujii, R. (2000). Effects of a kappa distribution function of electrons on incoherent scatter spectra. *Ann. Geophys.*, *18*(9), 1216–1223. https://doi.org/10.1007/s00585-000-1216-2

Schulz, M., and Lanzerotti, L. J. (1974). *Particle Diffusion in the Radiation Belts*. Berlin: Springer-Verlag.

Summers, D., and Thorne, R. M. (1992). A new tool for analyzing microinstabilities in space plasmas modeled by a generalized Lorentzian (Kappa) distribution. *J. Geophys. Res.: Space Phys.*, *97*(A11), 16827–16832. https://doi.org/10.1029/92JA01664

Vasyliunas, V. M. (1968). A survey of low-energy electrons in the evening sector of the magnetosphere with OGO 1 and OGO 3. *J. Geophys. Res.*, *73*(9), 2839–2884. https://doi.org/10.1029/JA073i009p02839

Viñas, A. F., Mace, R. L., and Benson R. F. (2005). Dispersion characteristics for plasma resonances of Maxwellian and Kappa distribution plasmas and their comparisons to the IMAGE/RPI observations. *J. Geophys. Res.: Space Phys.*, *110*(A6), A06202. https://doi.org/10.1029/2004JA010967

Xiao, F. L. (2006). Modelling energetic particles by a relativistic kappa-loss-cone distribution function in plasmas. *Plasma Phys. Controlled Fusion*, *48*(2), 203–213. https://doi.org/10.1088/0741-3335/48/2/003

Xiao, F. L., Shen, C. L., Wang, Y. M., Zheng, H. N., and Wang, S. (2008). Energetic electron distributions fitted with a relativistic kappa-type function at geosynchronous orbit. *J. Geophys. Res.: Space Phys.*, *113*(A5), A05203. https://doi.org/10.1029/2007JA012903

Xiao, F. L., Liu, S., Tao, X., Su, Z. P., Zhou, Q. H., Yang, C., He, Z. G., He, Y. H., Gao, Z. L., … Blake, J. B. (2017). Generation of extremely low frequency chorus in Van Allen radiation belts. *J. Geophys. Res.: Space Phys.*, *122*(3), 3201–3211. https://doi.org/10.1002/2016JA023561

Xue, S., Thorne, R. M., and Summers, D. (1993). Electromagnetic ion-cyclotron instability in space plasmas. *J. Geophys. Res.: Space Phys.*, *98*(A10), 17475–17484. https://doi.org/10.1029/93JA00790

Yang, Q. W., Yang, C., He, Y. H., Liu, S., Zhou, Q. H., and Xiao, F. L. (2016). Magnetospheric chorus wave instability induced by relativistic Kappa-type distributions. *Sci. China Technol. Sci.*, *59*(11), 1739–1745. https://doi.org/10.1007/s11431-016-0161-2

Zong, Q. G., Zhou, X. Z., Li, X., Song, P., Fu, S. Y., Baker, D. N., Pu, Z. Y., Fritz, T. A., Daly, P., ... Réme, H. (2007). Ultralow frequency modulation of energetic particles in the dayside magnetosphere. *Geophys. Res. Lett.*, *34*(12), L12105. https://doi.org/10.1029/2007GL029915